Supporting Information

Experimental Section

The synthesis of $Cu_{2-x}Se$:

20 mg of Se powder and 2 g of [Bmim] Cl were mixed and heated to 80 °C under stirring and maintained for 30 min. Then 19 mg of $NaBH_4$ and 10 mL of deionized water were added, and stirring was continued for another 10 min. After that, 28 mg of Cu powder was added into the above solution, and the autoclaves were sealed and maintained at 180 °C for 10 h. After accomplishing the reaction, we cooled the autoclave to room temperature naturally, and the product was separated by centrifugation, washed with distilled water and ethanol several times, and dried in a vacuum at 60 °C overnight.

The synthesis of $Cu_2O(SeO_3)$:

The synthetic $Cu_{2-x}Se$ is calcined in air at 500°C for 2 h.

Characterization of Catalysts

Powder X-ray diffraction (XRD) patterns were recorded on a D8 Venture (Bruker, Germany) using Cu Kα radiation (λ=1.5418 Å) in the range of 10-80° with a scanning speed of 5° min^{-1}. The morphology and structure of the samples were observed by scanning electron microscopy (SEM, JSM 7800F) and high-resolution transmission electron microscopy (HRTEM, FEI TecnaiG2 S-Twin) with a field emission gun operating at 200 kV. X-ray photoelectron spectroscopy (XPS, ESCALAB-250) was carried out with Thermo ESCA Lab 250 analyzer operating at constant analyzer power mode.

Electrochemical measurement

Electrochemical measurements were conducted at the CHI 660E electrochemical workstation (Shanghai Chenhua Apparatus, China) using a standard three-electrode system, with a rotating disk electrode (7 mm in diameter) as the working electrode, a platinum slice as the counter electrode, and a Ag/AgCl as the reference electrode in 0.5 M H_2SO_4. The working electrode was prepared by polishing it with 50 nm α-Al_2O_3 on a polishing cloth, then dropping 7 μL of the catalyst ink and drying it naturally. The catalyst ink was made by 0.005g adding 300 μL of deionized water and 200 μL of ethanol and 10 μL of Nafion solution, and then the solution was treated with ultrasonic for half an hour to make sure samples were well dispersed. The electrode was activated and the surface bubbles of it were removed by running cyclic voltammetry (CV). The HER curve was scanned from -0.9 to -0.2 V (vs Ag/AgCl) with a scan rate of 5 mV/s in 0.5 M H_2SO_4. Electrochemical impedance spectroscopy (EIS) was obtained at -0.6 V (vs Ag/AgCl) with frequencies ranging from 100 kHz to 0.1 Hz within an AC voltage

of 5 mV.

Density Functional Theory Calculations

The density function calculations were performed using Vienna ab initio simulation package (VASP) with the projector augmented-wave (PAW) method [1, 2]. The generalized gradient approximation (GGA) functional parametrized by Perde Burke-Ernzerh of (PBE) was employed to describe the exchange correlation potential [3]. A plane-wave energy cutoff of 400 eV was used and the energies and forces on each atom were converged to 10^{-4} eV and 0.05 eV/Å, respectively. A gamma-only point was used for the Brillouin zone integrations in geometry optimization.

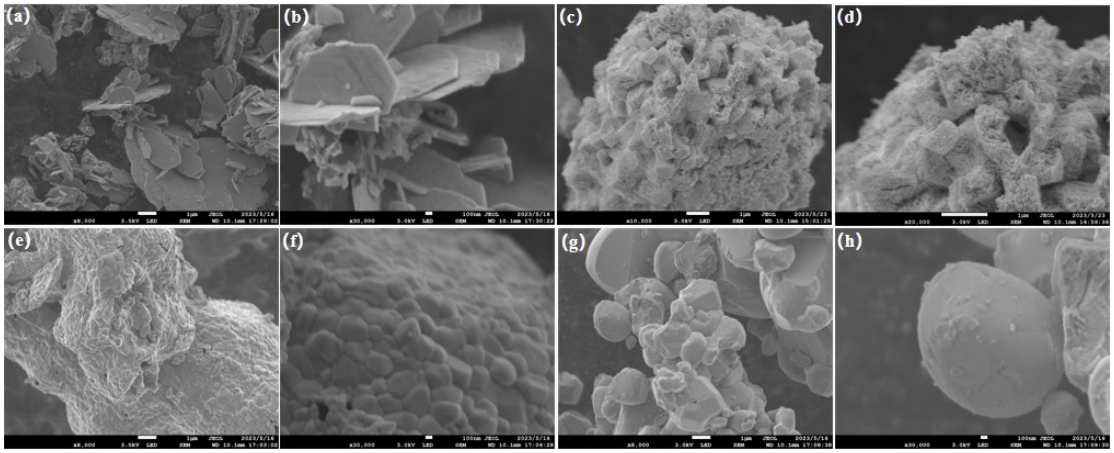

Fig. S1 SEM images of (a-b) $Cu_{2-x}Se$, (c-d) $Cu_2O(SeO_3)$, (e-f) CuO, and (g-h) Cu_2O.

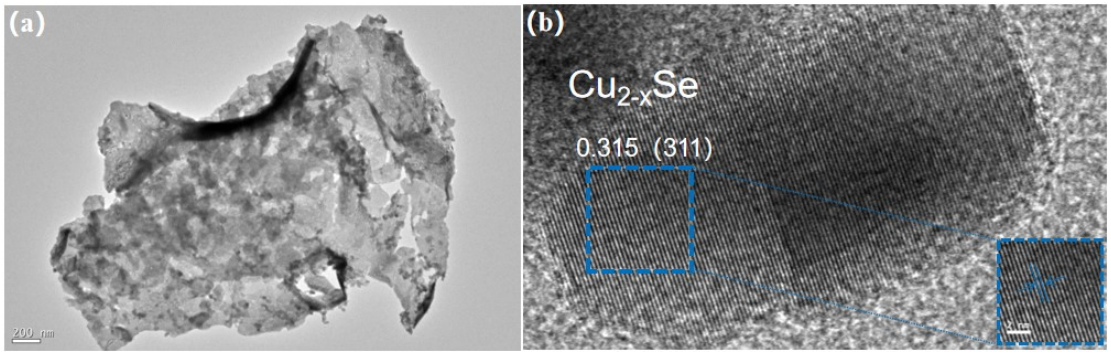

Fig. S2 TEM images of (a) $Cu_{2-x}Se$ and HRTEM images of (b) $Cu_{2-x}Se$.

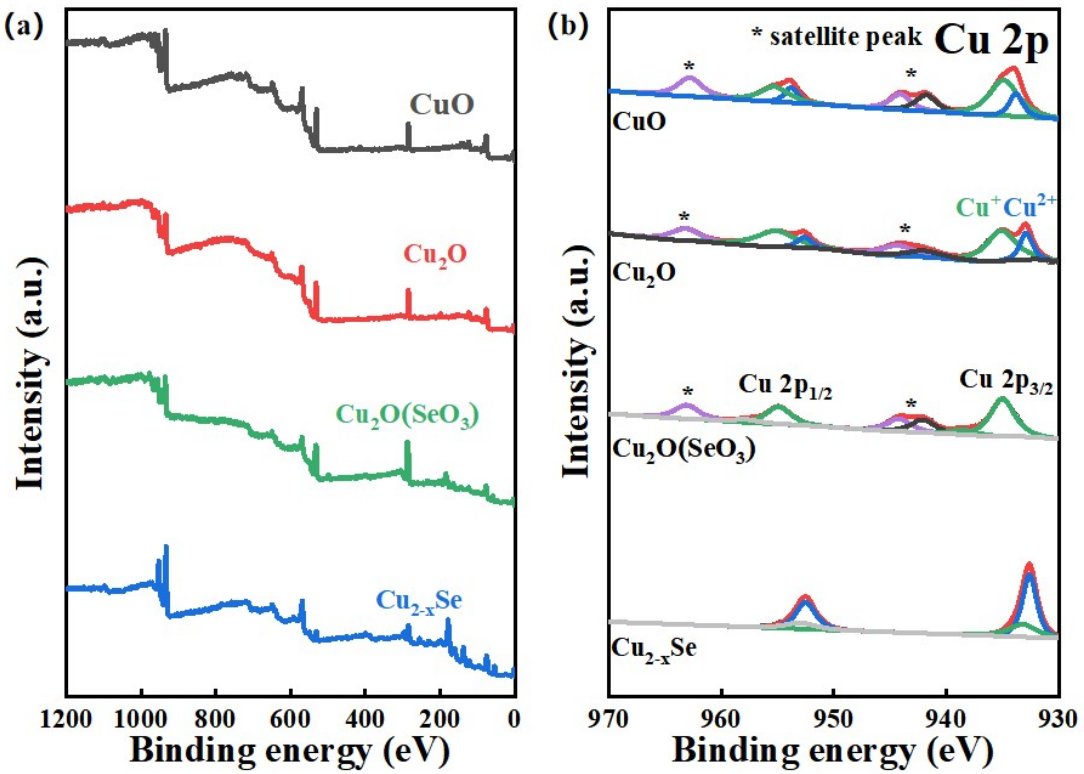

Fig. S3 XPS surface analysis of $Cu_{2-x}Se$, $Cu_2O(SeO_3)$, Cu_2O, and CuO. (a) Survey and (b) 2p.

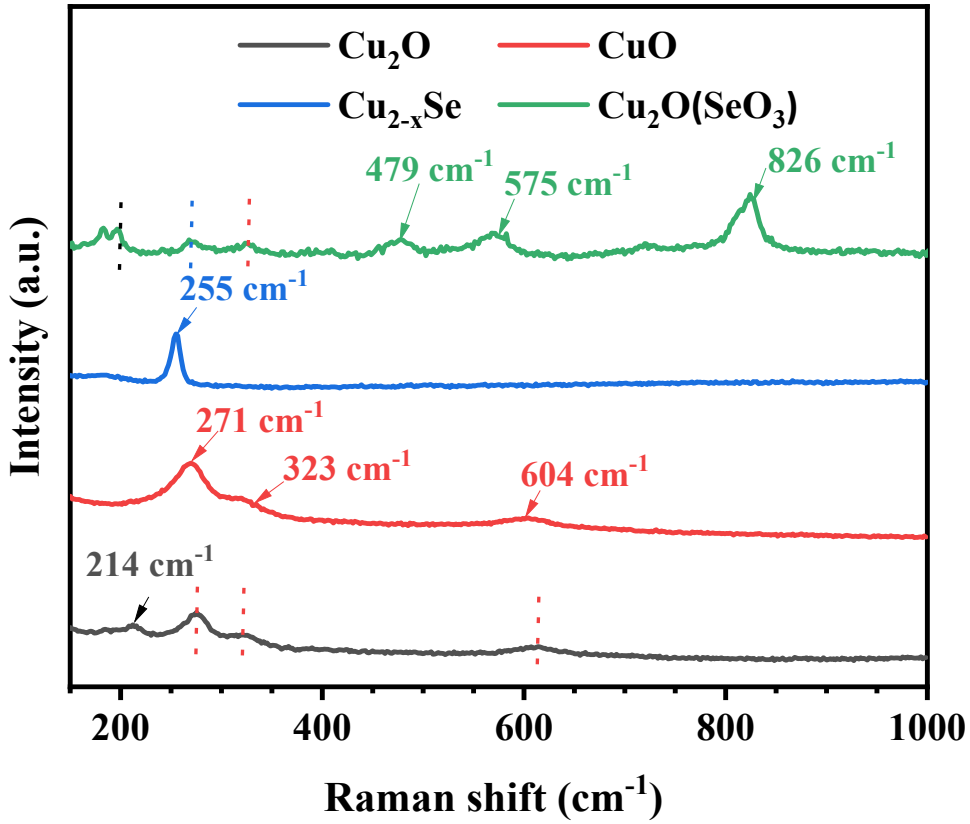

Fig. S4 The Raman of $Cu_2O(SeO_3)$, $Cu_{2-x}Se$, CuO, and Cu_2O.

A strong peak observed at 255 cm^{-1} can be assigned to the Se–Se stretching vibration in $Cu_{2-x}Se$, which is consistent with the previous reports. And the spectrum of CuO exhibits three main one-phonon modes at 271, 323 and 604 cm^{-1}, respectively. The peak at 271 cm^{-1} could be identified to the A_g mode of vibration, while the other two peaks at 323 and 604 cm^{-1} would be assigned to the B_g modes. The Raman peak observed at 214 cm^{-1} is from CuO. In addition, the strong peaks observed at 479 cm^{-1}, 575 cm^{-1} and 826 cm^{-1} of $Cu_2O(SeO_3)$ are identified to SeO_3. [3-10]

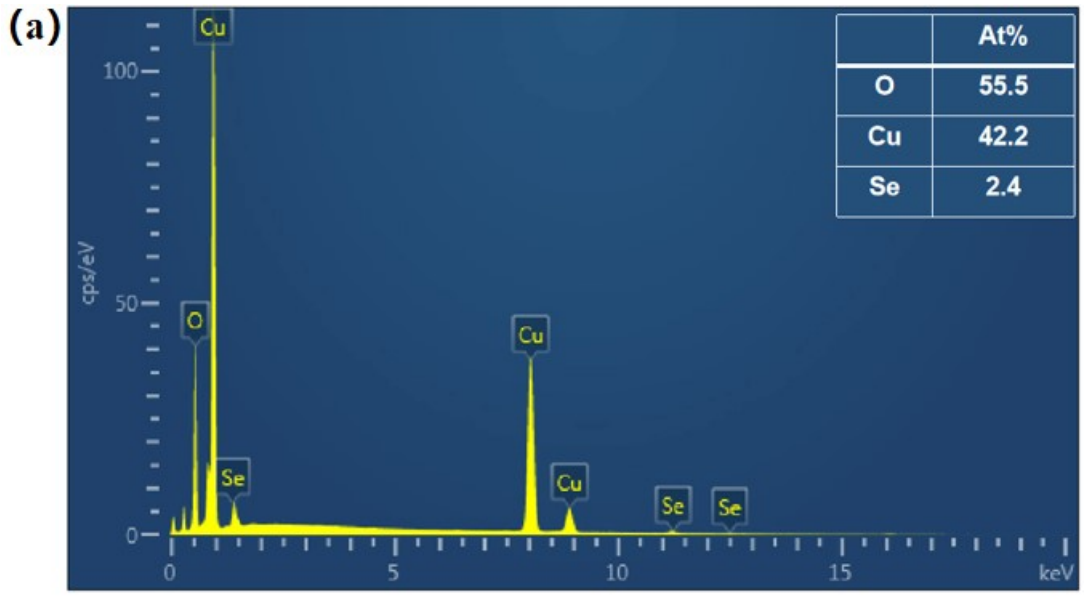

Fig. S5 EDS analysis for $Cu_2O(SeO_3)$.

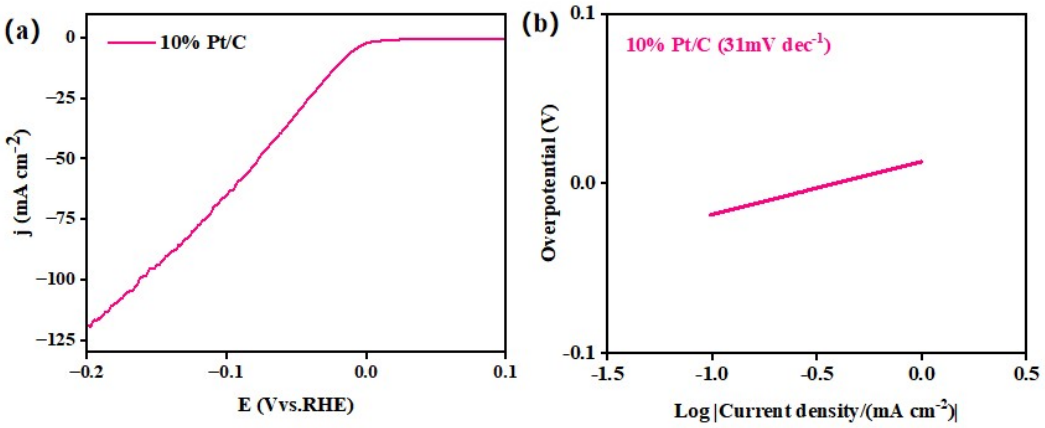

Fig. S6 (a) LSV curve and (b) corresponding Tafel plot of commercial 10% Pt/C.

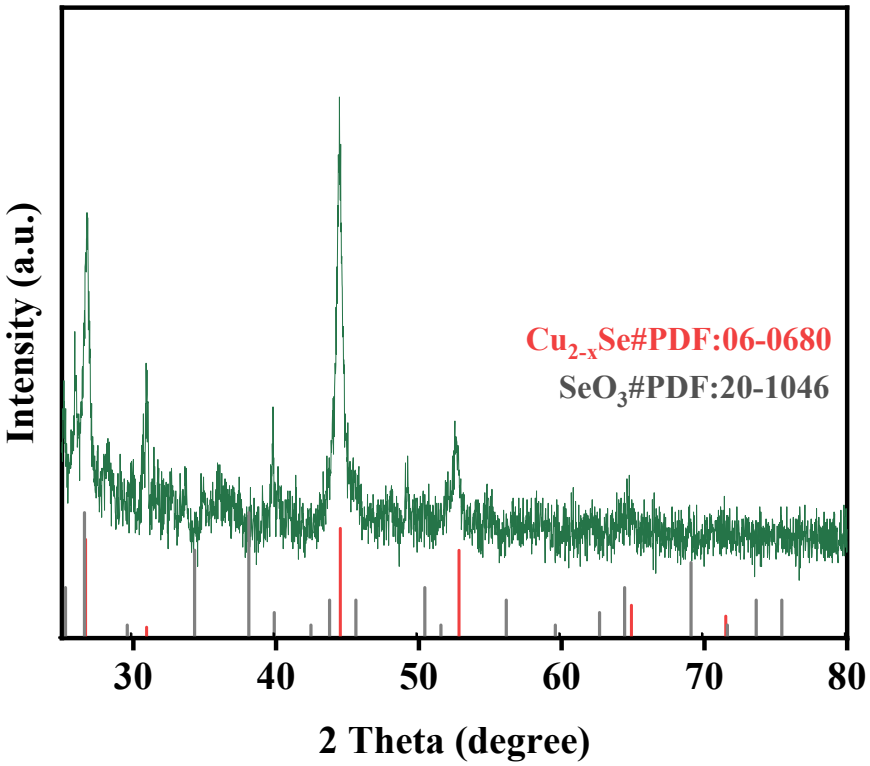

Fig. S7 The XRD of after testing $Cu_2O(SeO_3)$.

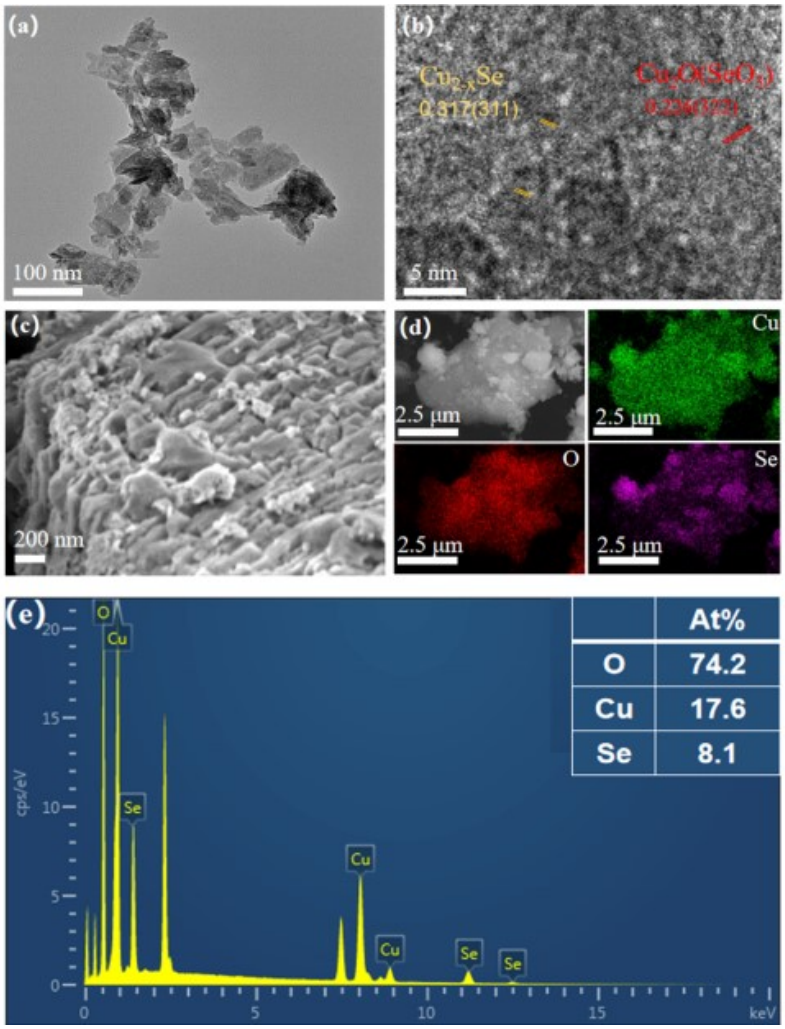

Fig. S8 (a-b) The TEM and HRTEM of after testing $Cu_2O(SeO_3)$. (c) The SEM of after testing $Cu_2O(SeO_3)$. (d-e) The EDS of after testing $Cu_2O(SeO_3)$.

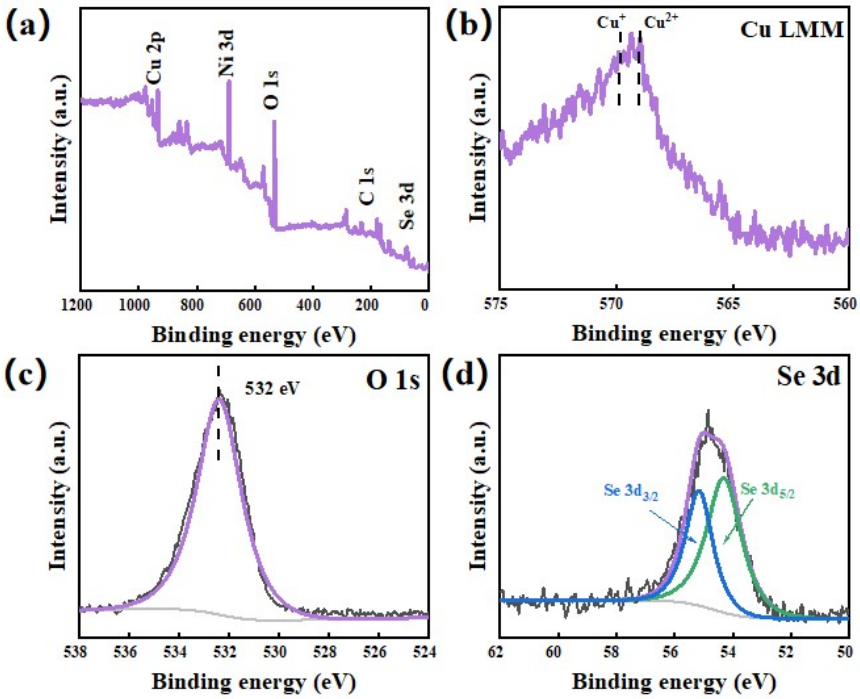

Fig. S9 (a-d) The XPS of after testing $Cu_2O(SeO_3)$.

Table S1 XPS and ICP results of $Cu_{2-x}Se$ and $Cu_2O(SeO_3)$.

	XPS		**ICP**	
	Element	**Atomic%**	**Element**	**Average value (ppm)**
$Cu_{2-x}Se$	Cu	41.2	Cu	28.3
	Se	29.3	Se	19.7
	O	29.5	/	/
$Cu_2O(SeO_3)$	Cu	21.6	Cu	30.6
	Se	11.7	Se	13.2
	O	66.7	/	/

Table S2 The performance comparison between $Cu_2O(SeO_3)$ and some recently reported Cu-based acidic HER catalysts.

Catalyst	**Current density (mA cm^{-2})**	**Overpotential (mV)**	**Tafel slope (mV dec^{-1})**	**Electrolyte**	**Reference**
$Cu_2O(SeO_3)$	10	438	136	0.5 M H_2SO_4	**This work**
OE_0-Cu	10	489	154	0.5 M H_2SO_4	*Langmuir.* **2022**, 3,9, 2993-2999.
$Cu_{2-x}Te$/wet	10	432	280	0.5 M H_2SO_4	*Inorg. Chem.* **2020**, 59, 15, 11129-11141.
CuS	10	449	171	0.5 M H_2SO_4	*Sci. Rep.* **2016**,61 ,6, 1-11.
Cu_2WS_4	10	462	140	0.5 M H_2SO_4	*Materials*. **2022**, 16, 1, 299.
Cu NA/CF	10	480	89	0.5 M H_2SO_4	*Nano Energy*. **2016**,30,858-866.
Cu NPs	10	530	132	0.5 M H_2SO_4	*Adv. Funct. Mater*. **2022**, 32, 18, 2112367
Cu foam	10	411	192	0.5 M H_2SO_4	*Adv. Funct. Mater*. **2022**, 32,18,2112367
$Cu_{2-x}Te$	10	454	183	0.5 M H_2SO_4	*J. Phys. Chem. Lett*. **2021**, 12,47, 11585-11590.
Cu NDs	10	442	108	0.5 M H_2SO_4	*Int. J. Hydrog. Energy*. **2021**, 46,2, 2007-2017.

Table S3 Comparison relating to the stability of different crystal planes.

	$Cu_{2-x}Se$		$Cu_2O(SeO_3)$	
Crystal planes	(111)	(311)	(111)	(322)
Energy (eV)	-322.76	-335.74	-531.75	-534.47

[1] S. Nosé, *J. Chem. Phys*., 1984, **81**, 511-519.
[2] G. Kresse and D. Joubert, *Phys. Rev*., B Condens. Matter, 1999, **59**, 1758-1775.
[3] J. Perdew, K. Burke and M. Ernzerhof, *Phys. Rev. Lett*., 1997, **77**, 386.
[4] K. Kremer and M. Johnsson, ***Inorg. Chem.***, 2018, **57**, 4640-4648.
[5] K. Denisova, P. Lemmens, D. Wulferding, P. Berdonosov, V. Dolgikh, A. Murtazoev, E. Kozlyakova, O. Maximova, A. Vasiliev, I. Shchetinin, F. Dolgushin, A. Iqbal, B. Rahaman and T. Saha-Dasgupta, ***J. Alloys Compd.***, 2022, **894**, 162291.
[6] A. M. Qadir and I. Y. Erdogan, *Int. J. Hydrog. Energy*, 2019, **44**, 18694-18702.
[7] K. R. Reddy, *J. Mol. Struct.*, 2017, **1150**, 553-557.
[8] E. Filippo, D. Manno and A. Serra, ***J. Alloys Compd***, 2012, **538**, 8-10.
[9] J. F. Xu, W. Ji, Z. X. Shen, W. S. Li, S. H. Tang, X. R. Ye, D. Z. Jia and X. Q. Xin, *J Raman Spectrosc*, 1999, **30**, 413-415.
[10] G. Jakubauskas, M. Gilic, E. Paluckiene, J. Mitric, J. Cirkovic, U. Ralevic, E. Usoviene, E. Griskonis and N. Petrasauskiene, *Chemosensors.,* 2022, **10**, 313.